Influence of Leading-Edge Thrust on Twisted and Cambered Wing Design for Supersonic Cruise

Harry W. Carlson* and David S. Miller*
NASA Langley Research Center, Hampton, Virginia

A study of leading-edge thrust phenomena at supersonic speeds has shown that although these forces are not large, they can be a significant factor in the design of wings for supersonic cruise. It is seen that the rather severe twisted and cambered wing surfaces resulting from the application of present design methods, which ignore leading-edge thrust, can be replaced by more moderate surfaces with little or no loss in aerodynamic efficiency if realistic possibilities for the attainment of some fraction of the theoretical thrust are taken into account.

Nomenclature

b	= wing span
c	= local wing chord
c_{av}	= wing average chord
$\bar{c}$	= wing mean aerodynamic chord
C_a	= section axial or chord force coefficient
C_A	= wing axial or chord force coefficient
C_D	= wing drag coefficient
ΔC_D	= wing drag coefficient due to lift
C_L	= wing lift coefficient
C_m	= wing pitching-moment coefficient
$C_{m,o}$	= wing pitching-moment coefficient at zero lift
C_n	= section normal force coefficient
C_p	= pressure coefficient
C_t	= section thrust coefficient
C_T	= wing thrust coefficient
$(L/D)_{max}$	= maximum lift-drag ratio
M	= Mach number
r	= leading-edge radius
R	= freestream Reynolds number based on $\bar{c}$
S	= wing area
t	= wing section maximum thickness
x,y,z	= Cartesian coordinates
x'	= distance behind wing leading edge
α	= angle of attack, deg
β	$= \sqrt{M_\infty^2 - 1}$
ΔC_p	= lifting pressure coefficient
Λ_{le}	= leading-edge sweep angle, deg

Introduction

LEADING-EDGE thrust, a factor of great importance in subsonic aerodynamics, has traditionally been ignored in supersonic wing design. It was commonly thought that leading-edge forces at supersonic speeds would be truly negligible for airfoil sections thin enough to prevent large wave drag penalties. With the realization that wing twist and camber could, in effect, substitute for leading-edge thrust and produce even higher theoretical levels of lifting efficiency,[1] efforts were concentrated on this more promising approach. A number of studies[2-5] of twisted and cambered wings with sharp leading edges which preclude any attainment of leading-edge thrust were conducted. Although the full theoretical benefits could not be realized, quite significant gains were achieved and wing twist and camber became a standard feature of supersonic cruise aircraft designs.

Presented as Paper 81-1656 at the AIAA Aircraft Systems and Technology Conference, Dayton, Ohio, Aug. 11-13, 1981; submitted Sept. 30, 1981; revision received July 8, 1982.

*Aero-Space Technologist, Supersonic Aerodynamics Branch, High-Speed Aerodynamics Division. Member AIAA.

Theoretically optimum camber surfaces given by typical numerical design methods,[6,7] however, are not easily incorporated into practical airplane designs. The large root chord angles and the resultant large cabin floor slopes are particularly troublesome. A possible remedy to this problem may lie in the achievement of some portion of the theoretical leading-edge thrust. If near theoretical leading-edge thrust could be attained over even a limited range of angle of attack or lift coefficient, the wing design-lift coefficient and the resultant camber surface severity could be reduced accordingly with little or no loss in aerodynamic efficiency. A new prediction method[8] now provides a means of estimating realistically attainable thrust for a wide variety of wing planforms and airfoil section shapes at specified Mach and Reynolds number operating conditions. A computer program[9] incorporates the leading-edge thrust calculations and also accounts for other aerodynamic nonlinearities which provide more realistic estimates of the aerodynamic characteristics of twisted and cambered wings. This paper will illustrate the use of the computer program[9] in combining the benefits of leading-edge thrust with the benefits of wing twist and camber to yield high levels of aerodynamic performance for wings of moderate camber surface severity.

Discussion

Leading-Edge Thrust

Theoretical drag-due-to-lift factors for arrow wings with full leading-edge thrust are shown in Fig. 1. The linearized theory portion of the computer program described in Ref. 9 was used to provide estimates for subsonic trailing-edge conditions which are not covered by the analytic expressions of Ref. 10. The accuracy of the numerical solutions for the high aspect ratio arrow wings is rather poor, but the faired curves should provide a reasonable estimate of the trends. For arrow wings with no leading-edge thrust, the drag-due-to-lift factors are nowhere lower than for the sonic leading-edge condition (where full-thrust and no-thrust factors are identical). Thus the potential benefit of leading-edge thrust is seen to be quite large. The figure also illustrates the benefits of large aspect ratios (or large notch ratios) and the approach to the aerodynamically ideal swept lifting line. For an infinite aspect ratio ($\cot\Lambda_{le}/\cot\Lambda_{te} = 1.0$), the drag-due-to-lift is zero for all sweep angles except zero.

The theoretical leading-edge thrust, however, is subject to severe limitations and often only small fractions of the potential thrust may be realized. The leading-edge force must be generated by local pressures acting on local surfaces. Wings suitable for supersonic cruise are typically very thin and thus the full theoretical thrust may require very large local pressures that are, in fact, unattainable. Figure 2 shows a typical idealized pressure distribution on an airfoil section

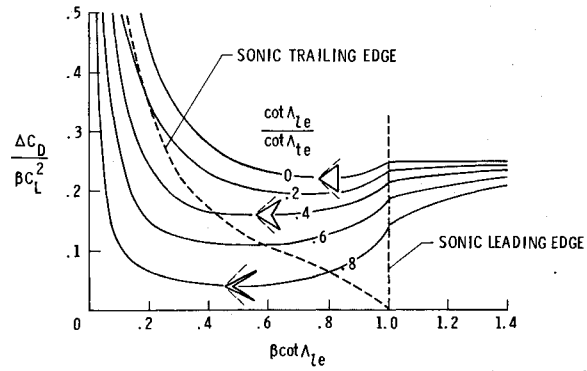

Fig. 1 Theoretical drag-due-to-lift factors for arrow wings with full leading-edge thrust as given by linearized theory.

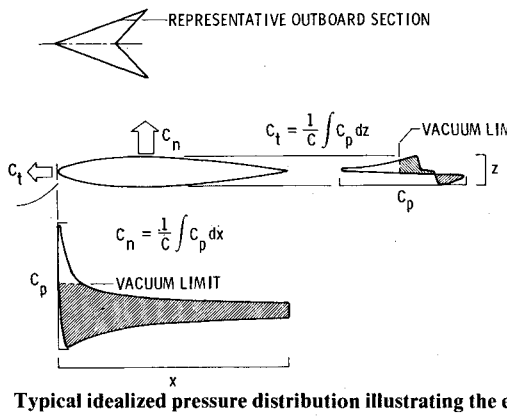

Fig. 2 Typical idealized pressure distribution illustrating the effect of realistic pressure limitations (section thickness exaggerated).

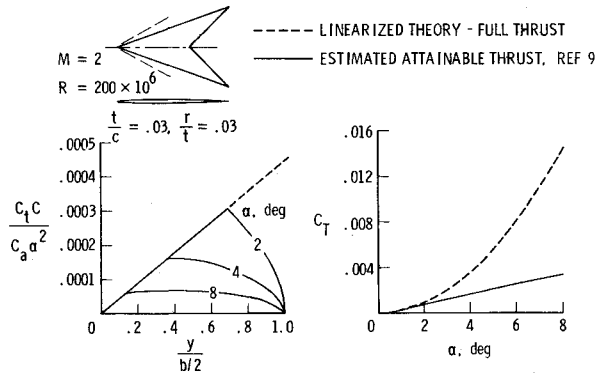

Fig. 3 Illustration of attainable thrust information provided by the method of Ref. 9.

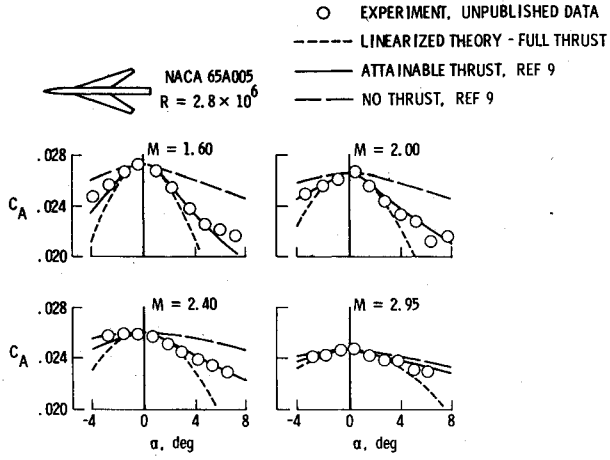

Fig. 4 Example of the estimation of attainable thrust by the method of Ref. 9.

of a wing with a subsonic leading edge. The effect of realistic pressure limitations (in this case the vacuum limit) on both normal force and chord force or thrust is illustrated by the shading. The normal force resulting from the indicated pressure integration is influenced to a relatively small degree by the truncation of pressures in excess of the vacuum limit. However, as shown here, the same pressure limitation can result in a net thrust that is only a small fraction of the unlimited thrust.

In Ref. 8, a study of the factors which place limits on the achievement of the theoretical thrust was made and an empirical method for estimation of attainable thrust was developed. The method is based on the use of simple sweep theory to permit a two-dimensional analysis, the use of theoretical airfoil programs to define thrust dependence on local geometric characteristics, and the examination of experimental two-dimensional data to define limitations imposed by local Mach and Reynolds numbers. An illustration of the attainable thrust information provided by the method as incorporated in the computing program of Ref. 9 is given in Fig. 3. The basic thrust data provided by the program are spanwise distributions of the estimated attainable thrust for a series of angles of attack. The wing may be of arbitrary planform and may be twisted and cambered. For convenience in comparison of the attainable thrust with full theoretical values the thrust parameter $C_t c/C_{av}\alpha^2$ is shown. These curves are numerically integrated in the program to provide estimates of the wing thrust coefficient as a function of angle of attack. As shown here, for very small angles of attack a large fraction of the theoretical thrust may be attainable even for relatively thin wings. However, the attainable fraction decreases markedly as the angle of attack is increased.

Because little attention has been given to supersonic cruise configurations with rounded wing leading edges, it is difficult to find data which display appreciable amounts of leading-edge thrust. A few examples are given in Ref. 10. Unpublished data shown in Fig. 4 served to demonstrate rather clearly a significant amount of thrust for Mach numbers up to 2.95. Axial or chord force coefficient plotted as a function of angle of attack as shown here is the best indicator of the presence or absence of leading-edge thrust. Perhaps one reason that leading-edge thrust was previously thought to be of so little significance at supersonic speeds is the rarity of the presentation of axial force data, which could have given the necessary clues. Linearized theory with leading-edge thrust ignored predicts no variation of axial force with angle of attack; but when the full thrust is included (the short dashed line) a large decrease in axial force, a function of the square of the angle of attack, is predicted. The nonlinear aerodynamic prediction method of Ref. 9 predicts a small decrease in axial force with increasing angle of attack due to a nonsymmetrical distribution of lifting forces over the whole of the airfoil; but the more important effect is due to the attainable thrust estimate. The estimate given by the method of Ref. 9 is seen to agree well with the experimental data. For this wing with a 5% thick section, more than half of the theoretical thrust is seen to be realized for angles of attack as high as 4 deg.

The data provided by the method of Ref. 10 permit attainable leading-edge thrust considerations to be included in tradeoff studies for optimization of supersonic wing design. An example with wing leading-edge radius as the variable is given in Fig. 5. The wing has a 70-deg swept leading-edge arrow planform and is assumed to be operating at a Mach number of 2 and a Reynolds number of 200 million. The basic wing section is a 3% thick circular arc. This was modified by the substitution of parabolic nose sections to provide a series of airfoils with different leading-edge radii. Leading-edge thrust and drag-due-to-lift factors were evaluated by the method of Ref. 9, but zero-lift wave drag was evaluated by the far-field wave drag method of Ref. 11. At the left of the figure, lift-drag polars are shown for three values of the leading-edge radius. Attainable thrust data from the method

of Ref. 9 are compared with linearized theory data (also from the method of Ref. 9). The linearized theory curve for no leading-edge thrust is almost identical to the nonlinear-method attainable thrust curve for $r/t=0$. The drag at zero-lift values which are indistinguishable in the plot are tabulated on the figure. The variation of the maximum lift-drag with leading-edge radius shown at the right of the figure indicates an appreciable increase in the maximum lift drag for relatively small wing section changes. The inset sketches show the first 10% of the streamwise profile. Even the largest r/t value of 0.03 shown here for which an L/D increase of 0.7 is indicated has a relatively minor effect on the overall section shape. Extrapolated data from wind-tunnel tests of a sharp leading-edge wing in this series is also shown. There is some evidence[10] that this wing actually produced a small amount of thrust at the test conditions. A leading-edge radius of absolutely zero can, of course, be only a mathematical concept.

An example of the use of the method of Ref. 9 to study the influence of wing planform on attainable thrust is shown in Fig. 6. A complex wing planform[12,13] (results given by solid line) is compared with three other planforms all having the same span, overall length, trailing-edge shape, leading-edge radius, maximum thickness, and location of maximum thickness with respect to the leading edge. Two of the comparison wing planforms have straight leading edges with leading-edge sweeps of 66.6 and 68.8 deg. The third comparison wing has exactly the same planform as the complex wing for the inboard region out to 43% of the span; from this span position to the wing tip, the leading edge has a constant 66-deg sweep. For each of the four planforms, attainable wing thrust as a function of wing lift is shown on the left of Fig. 6, and for a given lift coefficient, the spanwise variation of attainable wing section thrust is presented on the right of the figure. Although the study reported in Ref. 13 indicated that the complex planform would produce significant amounts of leading-edge thrust of supersonic speeds, the results in this figure show that other, and possibly less complex, planforms would produce even more thrust over a wide range of lift coefficients. The reason for this is primarily due to the amount of thrust produced on the outboard half of the wing. As shown in the figure, on the complex wing planform the thrust builds up quickly on the inboard region but falls off dramatically on the outboard region owing to the continuously decreasing sweep. The planforms with constant sweep do not produce as much thrust inboard but do not lose as much outboard; consequently, both constant-sweep planforms are overall better thrust producers than the original complex planform. The best thrust-producing wing was obtained by combining features of the complex and the straight leading-edge planforms; this resulted in a wing which, as shown in the figure, develops thrust quickly inboard and does not suffer severe thrust losses outboard. These results show that planform shaping can significantly affect the production of leading-edge thrust and that planform selection will definitely have an impact on the design of efficient thrust-producing wings.

The studies discussed herein and others reported in Refs. 8, 9, and 13 show that although leading-edge thrust effects at supersonic speeds may be small, they are by no means negligible. Thus the commonly accepted approach to the optimization of supersonic wing performance which relies exclusively on wing twist and camber while discounting any possibility of leading-edge thrust must be questioned. To begin this reexamination, it will be of interest to discuss the characteristics of optimized camber surfaces and to point out some similarities between wing surface shaping and leading-edge thrust as a means of achieving high levels of lifting efficiency.

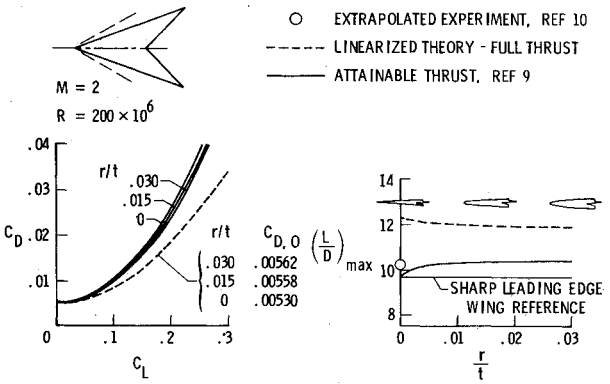

Fig. 5 Estimated effect of leading-edge radius on the aerodynamic efficiency of an uncambered wing.

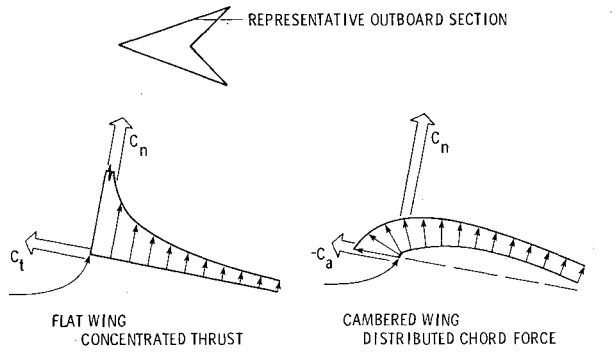

Fig. 7 Illustration of flat wing leading-edge thrust and the alternative distributed chord force on a twisted and cambered wing.

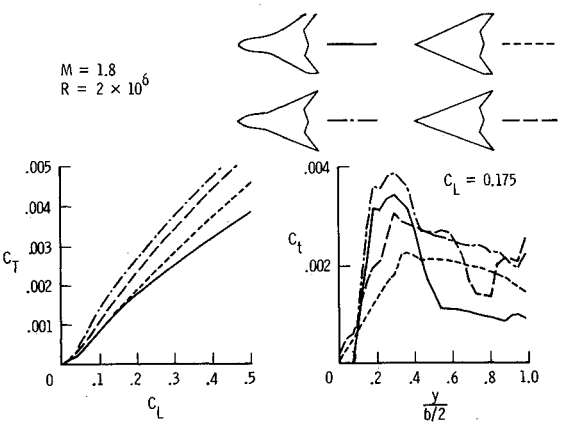

Fig. 6 Example of the use of the method of Ref. 9 to study the influence of planform on attainable thrust.

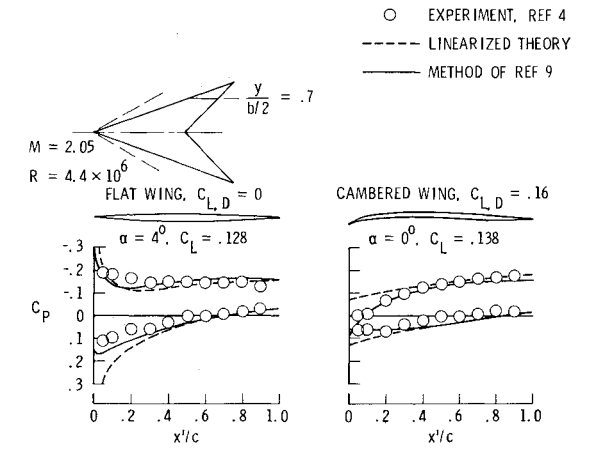

Fig. 8 Example of the failure to achieve linearized theory loadings in the wing leading-edge region.

Conventional Twisted and Cambered Wing Design

Twisted and cambered wing design is defined by allowing local portions of the wing to assume surface slopes and corresponding pressure loadings (subject to all mutual interference effects) which produce a wing surface with a minimum drag coefficient for a given lift coefficient. Often, as in the numerical methods of Refs. 6 and 7, the process is carried out by selection of an optimum combination of overall wing loadings. Although a properly designed twisted and cambered wing will normally display some degree of surface curvatures over the entire planform, the shaping is most pronounced in the immediate vicinity of the leading edge. The critical leading-edge shape and typical pressure loadings are illustrated in Fig. 7. This figure also offers an opportunity to compare the cambered wing performance benefits with those resulting from a theoretical concentrated leading-edge thrust force acting at the wing leading edge. Wing surface shapes, linearized theory pressure distributions, and the resultant force vectors are shown for representative outboard sections of a flat wing and a cambered wing of the same planform. The leading-edge thrust results from the upwash field ahead of the wing and the high local velocities and accompanying low pressures which occur as air flows around the wing leading edge to the upper surface from a stagnation point on the undersurface. For a flat wing airfoil section of zero thickness, the pressure at the leading edge is theoretically infinite (a mathematical singularity) but the resultant theoretical force remains finite. The cambered wing, in effect, replaces the leading-edge singularity with a distribution of finite pressures over a finite distance to provide a similar result. In this case, the surface slope at the leading edge is infinite but the pressure loading is finite. For a given planform, an optimum twist and camber distribution can produce a theoretical drag-due-to-lift factor slightly better than that for full theoretical leading-edge thrust; but there is generally a rather direct relationship between the two alternatives. Twisted and cambered wing benefits are very small for wings with supersonic leading edges which, of course, produce no thrust.

Real flow limitations on the attainment of the theoretical leading-edge thrust were discussed previously. In a similar fashion, real flow considerations limit the theoretical benefits of wing twist and camber. These limitations may be discussed with the aid of Fig. 8 which shows pressure distributions for typical outboard sections of a highly twisted and cambered wing and a flat wing of the same planform. Measured pressure distributions for 70-deg leading-edge sweep arrow wings at $M=2.05$ from Ref. 4 are compared with linearized theory predictions as given in that same reference and with predictions given by a new method incorporated in the computer program of Ref. 9. This new method accounts for nonlinearities in the relationship between pressure loadings and local surface slopes, predicts the attainment of leading-edge thrust, and provides an estimate of detached leading-edge vortex loadings that result when the full theoretical thrust forces are not totally realized. Data for the flat or uncambered wing show that, as might be expected, in the vicinity of the wing leading edge the linearized theory pressures are not achieved in the real flow. In a similar fashion, the linearized theory pressures in the vicinity of the leading edge of the twisted and cambered wing fail to be achieved. The cambered wing aerodynamic performance is particularly sensitive to this loss of lift because the design calls for it to act on the forward portion of the wing section to produce a resultant force with an appreciable thrust component. Because the nonlinear method data agree reasonably well with the experimental data, it will provide a better prediction of the effect of twist and camber on wing aerodynamics than does the linearized theory.

The failure of linearized theory methods to account for real flow effects such as those previously discussed has made it necessary to introduce some empiricism into twisted and

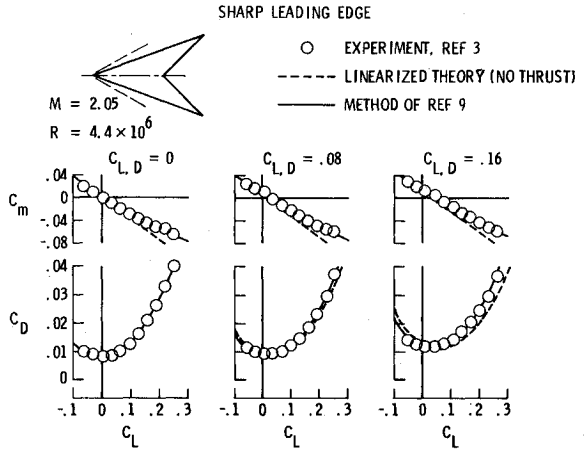

Fig. 9 Aerodynamic characteristics of wings with different camber surface severity (design-lift coefficient).

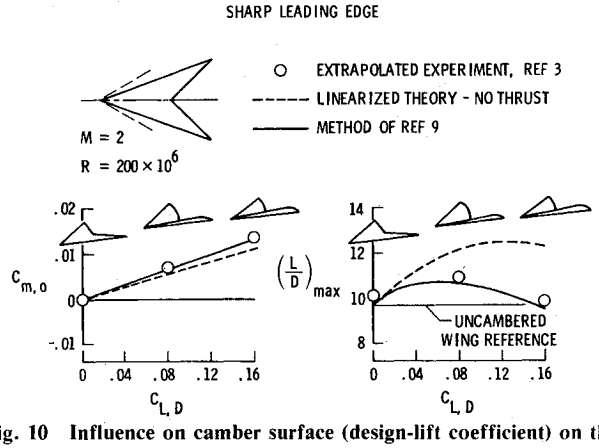

Fig. 10 Influence on camber surface (design-lift coefficient) on the aerodynamic characteristics of a sharp leading-edge wing.

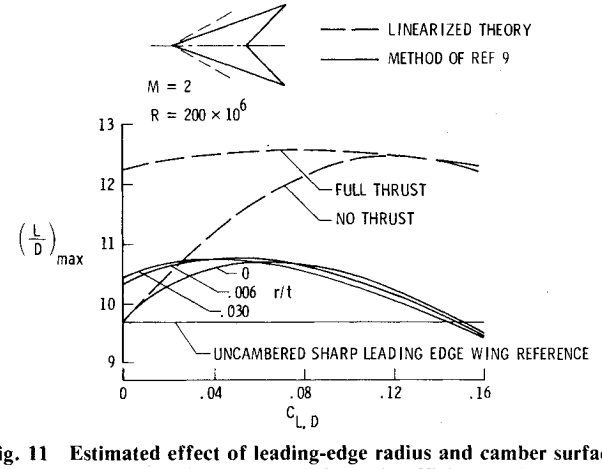

Fig. 11 Estimated effect of leading-edge radius and camber surface (design-lift coefficient) on the aerodynamic efficiency of an arrow wing.

cambered wing design. This has been accomplished by means of wind-tunnel data for wings with various degrees of twist and camber as governed by the design-lift coefficient. An example of such data for the 70-deg swept leading-edge arrow wing of Ref. 3 is shown in Fig. 9. Again, the experimental results are compared with both linearized theory and with the nonlinear method of Ref. 9. It is clear that the experimental drag levels of the twisted and cambered wings are considerably higher than the linearized theory predictions. There is also some failure to achieve the predicted pitching

moments. The variation of the key aerodynamic performance characteristics of maximum lift-drag ratio and pitching moment at zero lift are shown in Fig. 10. The self-trimming moment benefits, as predicted by linearized theory, vary linearly with design-lift coefficient and are almost as large as the experimental benefits. The experimentally measured maximum lift-drag ratio, however, does not follow the theoretical trends very closely and the actual benefit of twist and camber appears to maximize at somewhat less than one-half the theoretical benefit. From this and similar data (Ref. 5, for example), rules of thumb for application of twist and camber were devised. Generally, the wing design-lift coefficient is selected as from one-half to eight-tenths of the design-lift coefficient giving maximum theoretical benefits. The newer prediction method of Ref. 9 should provide a better means of selecting optimum twisted and cambered wing designs than does linearized theory.

Wing Design With Thrust Considerations

The only known data applicable to the establishment of rules for selection of design-lift coefficient is for sharp leading edges. The possibility of leading-edge thrust has thus been ignored. However, as mentioned previously, if near theoretical leading-edge thrust could be attained over even a limited range of angle of attack or lift coefficient, the wing design-lift coefficient and the resultant camber surface severity could be further reduced with little or no loss in aerodynamic efficiency.

Because the attained thrust predictions agree well with experimental data for uncambered wings with leading-edge bluntness and the nonlinear pressure loading predictions agree well with data for cambered wings with sharp leading edges, the method of Ref. 9 should be useful in selection of design-lift coefficient with thrust taken into account. An example of the use of this method in a study of the effects of camber surface severity is shown in Fig. 11. Predictions of the maximum lift-drag ratio for a 70-deg swept leading-edge arrow wing at a Mach number of 2 and a Reynolds number of 200 million are given as a function of the design-lift coefficients. The wing lifting surfaces were designed by means of a method described in Ref. 4 which was commonly employed before modern computer methods became available. Linearized theory results from that report indicate a peaking of the no-thrust $(L/D)_{max}$ curve at about 12.5 for a design-lift coefficient of about 0.125. According to linearized theory, the flat wing ($C_{L,D}=0$) with full leading-edge thrust would achieve an $(L/D)_{max}$ of about 12.24 at a lift coefficient of about 0.125. Note that the potential benefits of leading-edge thrust are reduced as the design-lift coefficient is increased. A well-designed twisted and cambered wing with a design-lift coefficient equal to the lift coefficient for the maximum lift-drag ratio has no potential for further improvements through leading-edge thrust. The linearized theory curves are for a wing with sharp leading-edge circular arc wing sections with a thickness to chord ratio of 3%. The method of Ref. 9 was used to analyze both that section and modifications thereto with leading-edge radius-to-maximum-thickness ratios of 0.0006 and 0.030. For the sharp leading-edge section, the nonlinear method predicts a maximum lift-drag ratio of about 10.7 for a design-lift coefficient of about 0.065. This result is consistent with previous observations in this paper and with experimental results from Ref. 5. The lift-drag ratio of about 10.7 is achieved at a lift coefficient of about 0.115 so that of the total lift, 56% is generated by the camber surface and 44% by additional flat surface lift. An increase in leading-edge radius to 3% of the maximum thickness is estimated to give a slight improvement in $(L/D)_{max}$ to 10.75; but even more important is the reduced wing camber as indicated by the reduction in design-lift coefficient to about 0.04. The $(L/D)_{max}$ occurs at a lift coefficient of about 0.11 and only about 36% of this lift is due to the camber surface. Thus it is seen that relatively small values of leading-edge radius could result in achievement of appreciable leading-edge thrust which, in turn, could permit significant reductions in camber surface severity. The SCAT 15-F supersonic cruise design of Ref. 14 employed a wing section with a rounded leading edge, but the design-lift coefficient was 80% of the cruise-lift coefficient—too high a value for leading-edge thrust to be of any significance at cruise conditions.

Other Design Considerations

This paper has been concerned only with wing-alone performance and the influence of attainable thrust on the design of the wing camber surface. Other considerations such as wing dihedral and shear for wings alone and fuselage and nacelle integration for complete configurations are treated in Refs. 15-18.

Concluding Remarks

A study of leading-edge thrust phenomena at supersonic speeds has shown that although these forces are not large, they can be a significant factor in the design of wings for supersonic cruise. It is seen that the rather severe twisted and cambered wing surfaces resulting from the application of present design methods, which ignore leading-edge thrust, can be replaced by more moderate surfaces with little or no loss in aerodynamic efficiency if realistic possibilities for the attainment of some fraction of the theoretical thrust are taken into account. The computer program which provides attainable thrust calculations and also accounts for other aerodynamic nonlinearities should prove to be valuable in tradeoff studies to balance and optimize the performance benefits of the twist and camber and the leading-edge thrust approaches.

References

[1] Brown, C.E. and McLean, F.E., "The Problems of Obtaining High Lift-Drag Ratios at Supersonic Speeds," *Journal of Aerospace Sciences*, Vol. 26, May 1959, pp. 298-302.

[2] Hallissy, J.M. Jr. and Hasson, D.F., "Aerodynamic Characteristics at Mach Numbers 2.36 and 2.87 of an Airplane Configuration Having a Cambered Arrow Wing With a 75-deg Swept Leading Edge," NACA RM L58E21, 1958.

[3] Carlson, H.W., "Aerodynamic Characteristics at Mach Number 2.05 of a Series of Highly-Swept Arrow Wings Employing Various Degrees of Twist and Camber," NASA TM X-332, 1960.

[4] Carlson, H.W., "Pressure Distributions of Mach Number 2.05 on a Series of Highly-Swept Arrow Wings Employing Various Degrees of Twist and Camber," NASA TN D-1264, 1962.

[5] Mack, R.J., "Effects of Leading-Edge Sweep Angle and Design Lift Coefficient on Performance of a Modified Arrow Wing at a Design Mach Number of 2.6," NASA TN D-7753, 1974.

[6] Carlson, H.W. and Middleton, W.D., "A Numerical Method for the Design of Camber Surfaces of Supersonic Wings With Arbitrary Planforms," NASA TN D-2341, 1964.

[7] Carlson, H.W. and Miller, D.S., "Numerical Methods for the Design and Analysis of Wings at Supersonic Speeds," NASA TN D-7713, 1974.

[8] Carlson, H.W., Mack, R.J., and Barger, R.L., "Estimation of Attainable Leading-Edge Thrust for Wings at Subsonic and Supersonic Speeds," NASA TP-1500, 1979.

[9] Carlson, H.W. and Mack, R.J., "Estimation of Wing Nonlinear Aerodynamic Characteristics at Supersonic Speeds," NASA TP-1718, 1980.

[10] Puckett, A.E. and Stewart, H.J., "Aerodynamic Performance of Delta Wings at Supersonic Speeds," *Journal of Aeronautical Science*, Vol. 14, Oct. 1947, pp. 567-587.

[11] Harris, Roy V. Jr., "An Analysis and Correlation of Aircraft Wave Drag," NASA TM X-947, 1964.

[12] Robins, A.W., Lamb, M., and Miller, D.S., "Aerodynamic Characteristics at Mach Numbers of 1.5, 1.8, and 2.0 of a Blended Wing-Body Configuration With and Without Integral Canards," NASA TP-1427, 1979.

[13] Robins, A.W. and Carlson, H.W., "High-Performance Wings With Significant Leading-Edge Thrust at Supersonic Speeds," *Journal of Aircraft*, Vol. 17, June 1980, pp. 419-422.

[14] Morris, O.A. and Fournier, R.H., "Aerodynamic Characteristics at Mach Numbers 2.30, 2.60, and 2.96 of a Supersonic Transport Model Having a Fixed, Warped Wing," NASA TM X-1115, 1965.

[15] Carlson, H.W. and McLean, F.E., "Current Methods for Prediction and Minimization of Lift-Induced Drag at Supersonic Speeds," NASA TM X-1275, 1966 (declassified October 20, 1976).

[16] Robbins, A.W., Morris, O.A., and Harris, R.V. Jr., "Recent Research Results in the Aerodynamics of Supersonic Vehicles," *Journal of Aircraft*, Vol. 3, Nov.-Dec. 1966, pp. 573-577.

[17] Baals, D.D., Robins, A.W., and Harris, R.V. Jr., "Aerodynamic Design Integration of Supersonic Aircraft," *Journal of Aircraft*, Vol. 7, Sept.-Oct. 1970, pp. 385-394.

[18] Carlson, H.W. and Harris, R.V. Jr., "A Unified System of Supersonic Aerodynamic Analysis, Analytic Methods in Aircraft Aerodynamics," NASA TP-228, 1970, pp. 639-658.